

Supporting Information

Free-standing MoS_x-based Dual Functional Polysulfide Catalyzer and Immobilizer for High Performance Li-S Batteries

Binchao Shi, Yue Wang, Chenxing Zhang, Xianhe Chen, Ertai Liu, Shilin Mei,* and Chang-Jiang Yao*

State Key Laboratory of Explosion Science and Technology, Beijing Institute of Technology,
Beijing 100081 P. R. China.

* E-mail: shilin.mei@bit.edu.cn; cjyao@bit.edu.cn

Synthesis of PPy@CP.

Carbon paper (CP, Toray Industries, Inc) was immersed in concentrated nitric acid, acetone and deionized water for ultrasonication (15 min) before electropolymerization to remove surface impurities. The stainless steel mesh (2 × 3 cm in size) as anode and carbon plate as cathode were inserted into the solution containing 0.267 M dibasic sodium phosphate, 0.26 M sodium dihydrogen phosphate, 0.1 M p-toluenesulfonic acid monohydrate and 0.092 M pyrrole. In chronopotentiometry, the stainless steel mesh was supplied with a current of 2 mA/cm², and the whole electropolymerization process lasted for 1 h. Then the stainless steel mesh was replaced with carbon paper for a second electropolymerization for 2 h. In order to remove the oxygen in the solution, argon was introduced to bubble for about 20 min. The obtained PPy@CP

was washed with deionized water several times. Finally, the obtained PPy@CP was cut into discs with a diameter of 12 mm.

Synthesis of MoS₃@PPy@CP and 1T & 2H MoS₂@CWs@CP.

PPy@CP discs was immersed in 5 mg/ml (NH₄)₂MoS₄ solution to adsorb MoS₄²⁻ ions under slow stirring for 12 h. Then 1 M HCl was added drop by drop under stirring until PH is about 3 and the mixture was stirred for 2 h. The MoS₃@PPy@CP was obtained and cleaned several times with deionized water until the pH was around 7.0 then dried at 60 °C under vacuum for 24 h. 1T & 2H MoS₂@CWs@CP can be obtained by heating MoS₃@PPy@CP at 500 °C for 2 h with a heating rate of 2 °C min⁻¹ under argon atmosphere.

Characterization.

X-ray diffraction (XRD) patterns of the obtained samples were characterized by a D8-Advance X-ray diffraction with Cu K α radiation. The morphological characterization of the obtained samples was performed by FESEM (HITACHI S-8230) with an energy dispersive X-ray spectrometer (EDS) and TEM (JEM-2100F). X-ray photoelectron spectroscopy (XPS) was measured on a Thermo Scientific K-Alpha. Thermal gravimetric analysis (TGA) was carried out with NETZSCH STA449F3 at a heating rate of 10 °C min⁻¹ from 30 to 900 °C in air atmosphere. Raman spectra were obtained by a Raman microscope (HORIBA Scientific LabRAM HR Evolution) with a laser excitation wave length of 633 nm.

Li₂S₆ permeation tests.

A symmetrical H-shaped pipe was used to carry out the permeability experiment. A certain amount of 0.05 M Li_2S_6 solution was added in one side of the chamber, and the same amount of DOL and DME solution (the DOL:DME ratio of 1:1 by volume) without Li_2S_6 was added in the other side of the chamber. 1T & 2H $\text{MoS}_2@\text{CWs}@\text{CP}$, $\text{MoS}_3@\text{PPy}@\text{CP}$, and the simultaneous used of 1T & 2H $\text{MoS}_2@\text{CWs}@\text{CP}$ plus $\text{MoS}_3@\text{PPy}@\text{CP}$ were tested under the supporting of commercial Celgard separator.

Symmetric cell assembly.

In a symmetric cell, both the cathode and anode are of the same material (1T & 2H $\text{MoS}_2@\text{CWs}@\text{CP}$ or $\text{MoS}_3@\text{PPy}@\text{CP}$). 20 μL Li_2S_6 electrolyte (containing 1 M LiTFSI, 1 wt% LiNO_3 , and 0.4 M Li_2S_6 in DOL/DME solution with a volume ratio of 1:1) and 20 μL reference electrolyte (containing 1 M LiTFSI, 1 wt% LiNO_3 in DOL/DME solution with a volume ratio of 1:1) were added to the cathode and anode of a standard 2032 coin cell, respectively. CV tests were conducted at various scan rates within the voltage range of -1.0 - 1.0 V (vs Li^+/Li).

Kinetics of Li_2S precipitation.

The obtained 1T & 2H $\text{MoS}_2@\text{CWs}@\text{CP}$, $\text{MoS}_3@\text{PPy}@\text{CP}$ as sulfur host with Li foil as the counter electrode were assembled into the 2032 coin cell. 20 μL Li_2S_8 (0.25 M) solution with 1.0 M LiTFSI in solvent of DOL and DME (1:1 v/v) was added to the 1T & 2H $\text{MoS}_2@\text{CWs}@\text{CP}$ cell, $\text{MoS}_3@\text{PPy}@\text{CP}$ cell, respectively. 20 μL electrolyte without Li_2S_8 was used as control anolyte. The assembled batteries were galvanostatically discharged to 2.12 V at 0.1 C, and then potentiostatically discharged at 2.05 V for 65 000 s.

Electrochemical characterization.

The 1T & 2H MoS₂@CWs@CP battery was composed of 1T & 2H MoS₂@CWs@CP (12 mm in diameter) with Li₂S₆ (15 μ l, 0.4 M, corresponding to 1.0 mg cm⁻² of elemental sulfur) as cathode. The MoS₃@PPy@CP battery was composed of carbon paper with the same amount of Li₂S₆ as cathode, MoS₃@PPy@CP as interlayer. The combined battery was composed of 1T & 2H MoS₂@CWs@CP with the same amount of Li₂S₆ as cathode, and MoS₃@PPy@CP as interlayer. All batteries were equipped with lithium metal foils as anode, Celgard 2325 as separator, and the 1,3-dioxolane and dimethoxyethane (1:1 volume) solution containing 1 M LiTFSI and 1 wt% lithium nitrate as electrolyte. The coin cell (CR2032) were assembled in the glove box with oxygen and water content below 0.01 ppm. CV and EIS measurements were performed on CHI660D electrochemical workstation (CHI instrument). The EIS test was conducted at an open circuit potential with a frequency range of 100 kHz to 0.01 Hz. Galvanostatic charge-discharge cycles were tested by LAND CT2001A instrument (Wuhan Jinnuo Electronic Co. Ltd.) in the potential range of 1.8-2.8 V at different discharge/charge current densities of 0.1-2 C (1 C=1675 mAh g⁻¹).

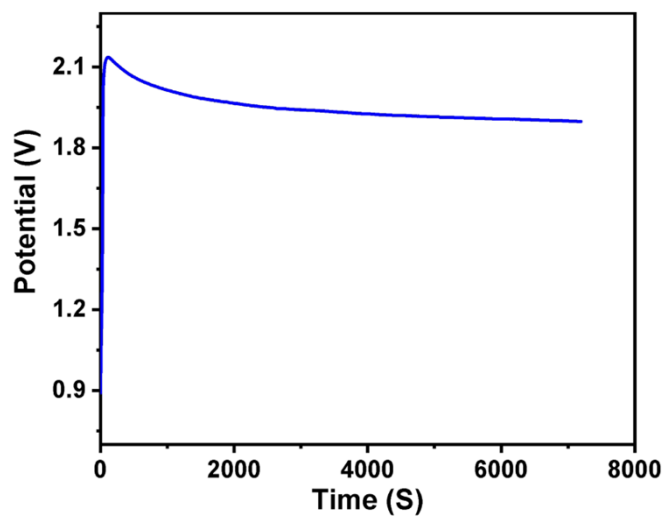


Fig. S1. Electropolymerization curve of pyrrole.

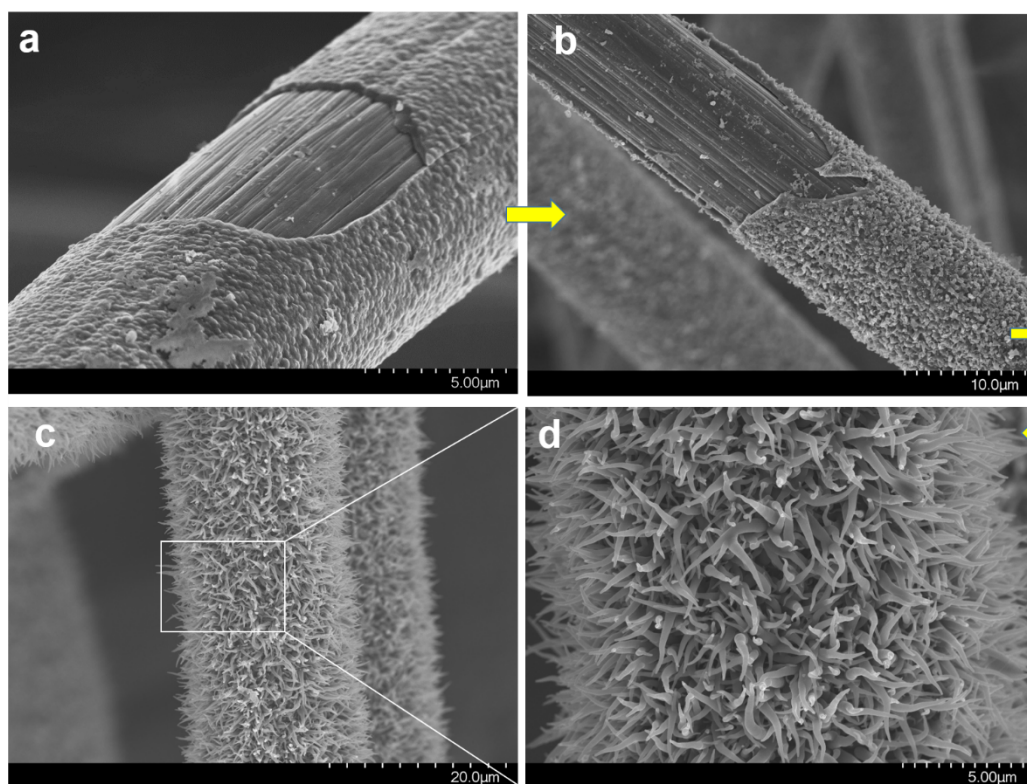


Fig. S2. The in situ growth process of PPy nanowires: morphologies captured at different electropolymerization time from 5 min to 40 min.

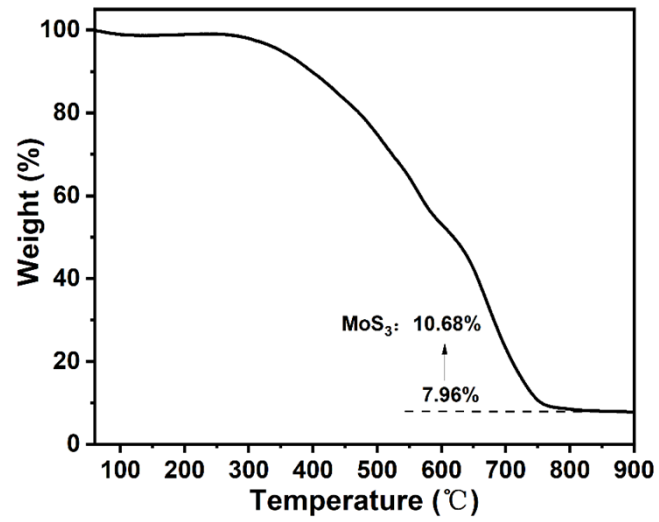


Fig. S3. TGA measurement of the MoS₃@PPy@CP material (in air atmosphere).

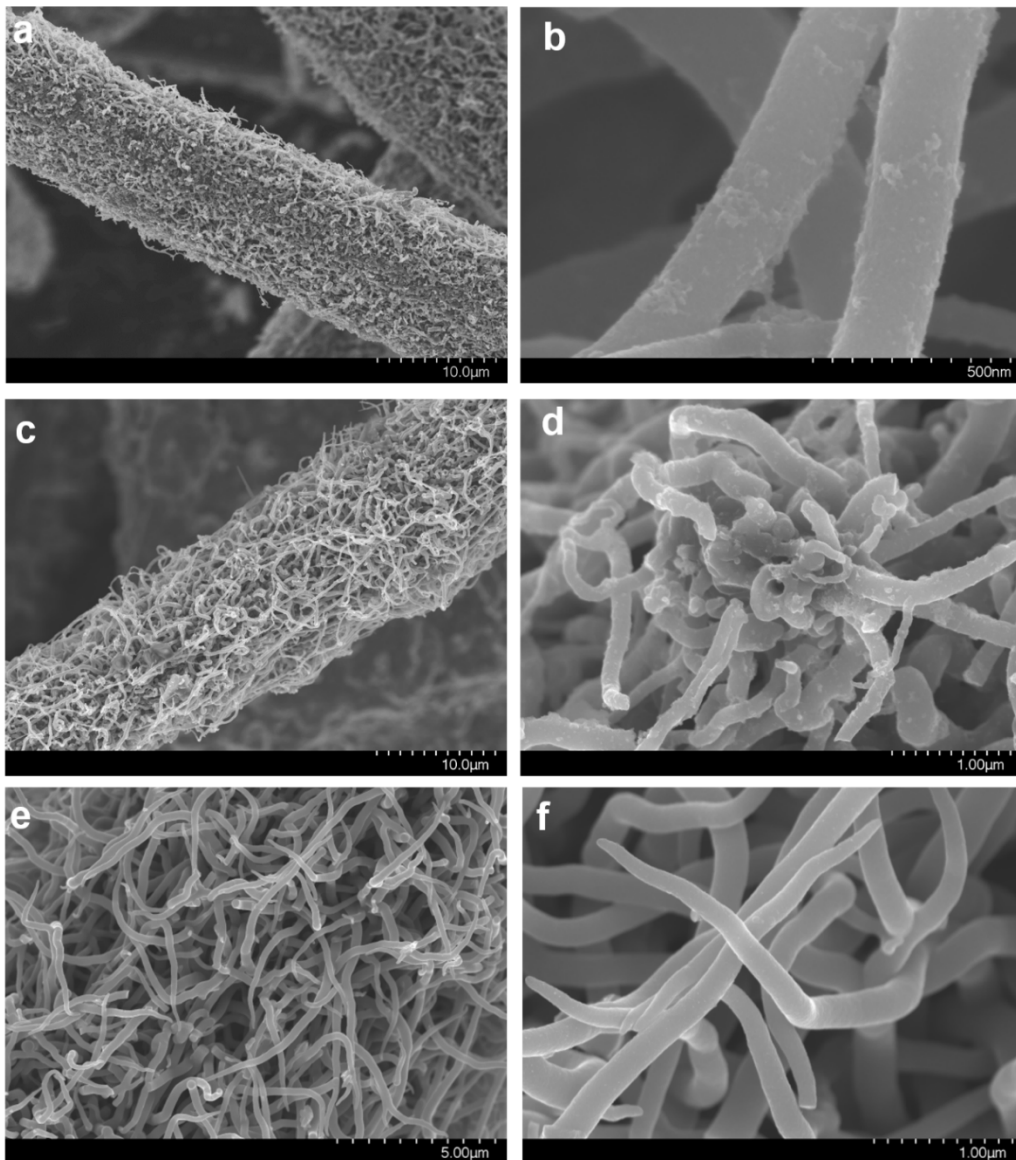


Fig. S4. SEM images of $\text{MoS}_3@\text{PPy}@\text{CP}$ (a, b), 1T & 2H $\text{MoS}_2@\text{CWs}@\text{CP}$ (c, d), and the CWs reference without MoS_2 (e, f).

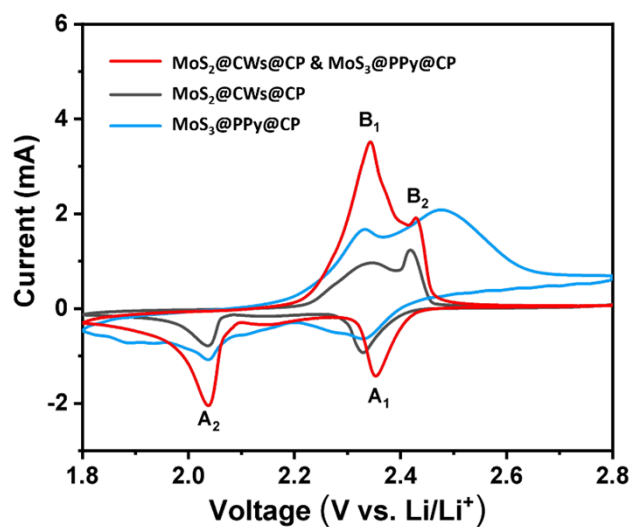


Fig. S5. CV curves of Li-S battery with the 1T & 2H $\text{MoS}_2@\text{CWs}@\text{CP}$, $\text{MoS}_3@\text{PPy}@\text{CP}$, and the 1T & 2H $\text{MoS}_2@\text{CWs}@\text{CP}$ & $\text{MoS}_3@\text{PPy}@\text{CP}$ at 0.1 mV s^{-1} .

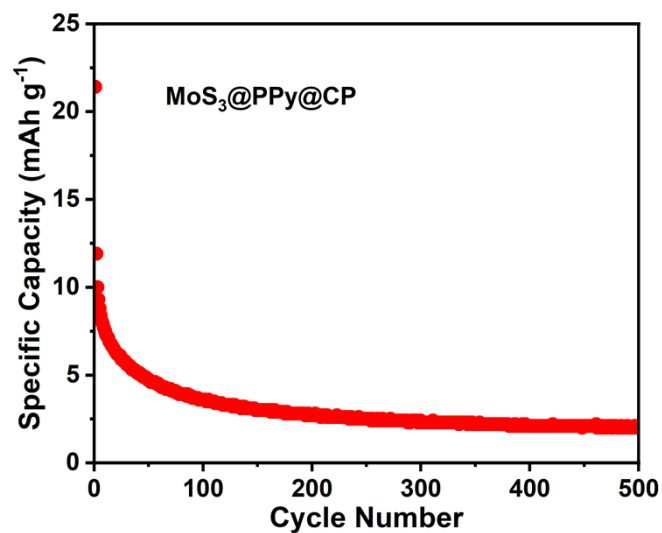


Fig. S6. $\text{MoS}_3@\text{PPy}@\text{CP}$'s capacity contribution at 0.2 C.

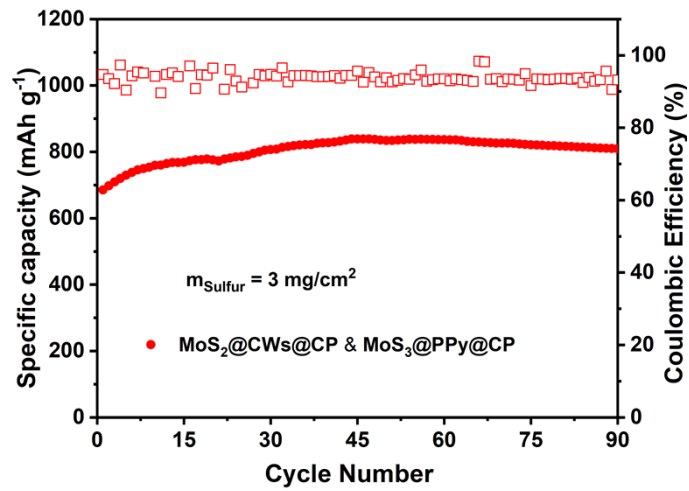


Fig. S7. Electrochemical performances of the three types of batteries with a sulfur loading of 3 mg cm^{-2} at 0.2 C .

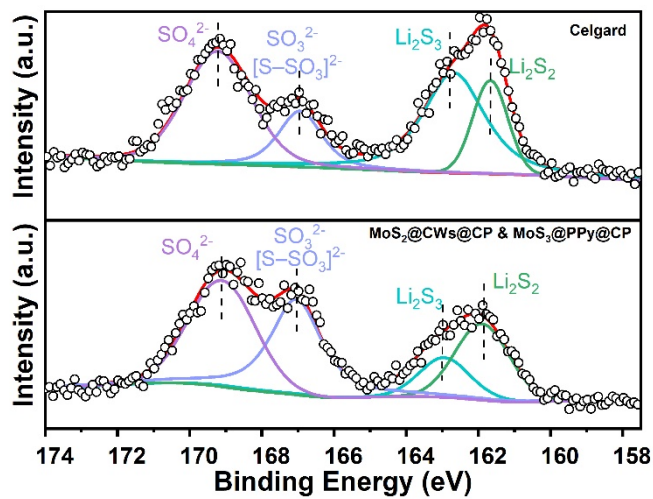


Fig. S8. XPS spectra of the surface components of Li metal anode after 200 cycles at 1 C .

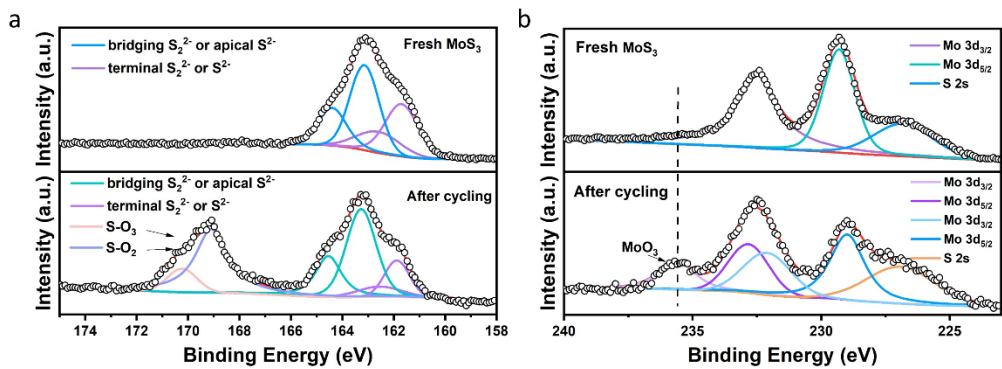


Fig. S9. XPS spectra of the MoS₃@PPy@CP before (a) and after cycling (b).

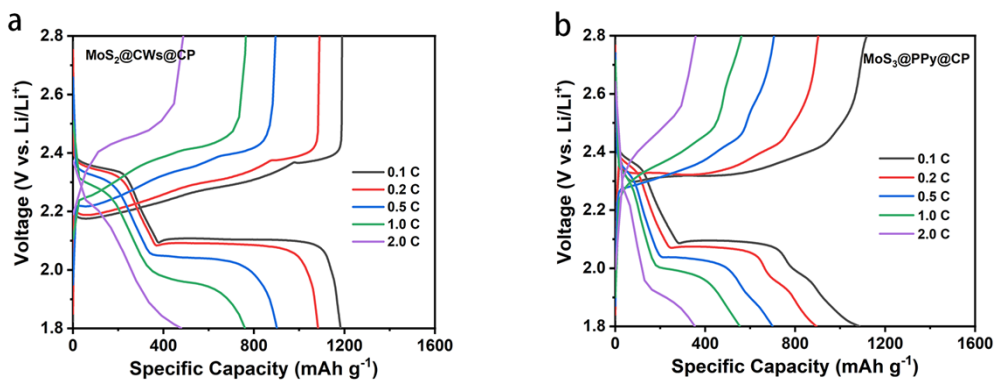


Fig. S10. Charge/discharge profiles of 1T & 2H MoS₂@CWs@CP and MoS₃@PPy@CP from 0.1 to 2 C.

Table S1. Capacity comparison of rate performance for 1T & 2H MoS₂@CWs@CP, MoS₃@PPy@CP, and 1T & 2H MoS₂@CWs@CP & MoS₃@PPy@CP

Electrodes	Discharge capacities (mAh g ⁻¹)					Recovered discharge capacities
	0.1 C	0.2 C	0.5 C	1 C	2 C	(mAh g ⁻¹) 0.2 C
1T & 2H MoS ₂ @CWs@CP	1172	1056	931	785	473	1032
MoS ₃ @PPy@CP	1086	897	714	553	350	928
1T & 2H MoS ₂ @CWs@CP & MoS ₃ @PPy@CP	1497	1357	1037	909	755	1324

Table S2. Comparison of cyclic performance for 1T & 2H MoS₂@CWs@CP, MoS₃@PPy@CP, and 1T & 2H MoS₂@CWs@CP & MoS₃@PPy@CP at 1 C

Electrodes	Initial capacity (mAh g ⁻¹)	200 th capacity (mAh g ⁻¹)	500 th capacity (mAh g ⁻¹)	Capacity retention (%)	Capacity decay per cycle (%)
1T & 2H MoS ₂ @CWs@CP	688	621	334	48.5 %	0.103 %
MoS ₃ @PPy@CP	743	570	451	60.7 %	0.078 %
1T & 2H MoS ₂ @CWs@CP & MoS ₃ @PPy@CP	821	758	678	82.6%	0.035 %

Table 3. A summary of the electrochemical performances of representative works.

Materials	Sulfur loading (mg cm ⁻²)	Initial capacity (mAh g ⁻¹)	Retained capacity (mAh g ⁻¹)	Cycle number	Capacity retention (%)	Capacity decay per cycle (%)	Current density	Ref
3S-TiO _{2-x} HoMSs	0.3	903	713	1000	79	0.021	0.5 C	1
PCNF-2	2.15	839.3	642.1	300	76.5	0.078	1 C	2
G@POF-Fe	1.33	1065	671	500	63.0	0.074	0.5 C	3
1T-MoS ₂ @CFC	1.2-1.4	828	497	400	60.02	0.10	0.5 C	4
Co-N-C	1.0	1161	850	300	73.2	0.10	0.5 C	5
1T & 2H MoS₂@CWs @CP & MoS₃@PPy @CP	1.0	821	678	500	82.6	0.035	1 C	This work

References

- [1] E. H. M. Salhabi, J. Zhao, J. Wang, M. Yang, B. Wang and D. Wang, Hollow Multi-Shelled Structural TiO_{2-x} with Multiple Spatial Confinement for Long-Life Lithium-Sulfur Batteries, *Angewandte Chemie International Edition*, 2019, **58**, 9078-9082.
- [2] F. Hu, H. Peng, T. Zhang, W. Shao, S. Liu, J. Wang, C. Wang and X. Jian, A lightweight nitrogen/oxygen dual-doping carbon nanofiber interlayer with meso-/micropores for high-performance lithium-sulfur batteries, *Journal of Energy Chemistry*, 2021, **58**, 115-123.
- [3] J.-L. Qin, B.-Q. Li, J.-Q. Huang, L. Kong, X. Chen, H.-J. Peng, J. Xie, R. Liu and Q. Zhang, Graphene-based Fe-coordinated framework porphyrin as an interlayer for lithium-sulfur batteries, *Materials Chemistry Frontiers*, 2019, **3**, 615-619.
- [4] D. Chen, W. Zhan, X. Fu, M. Zhu, J. Lan, G. Sui and X. Yang, High-conductivity 1T-MoS₂ catalysts anchored on a carbon fiber cloth for high-performance lithium-sulfur batteries, *Materials Chemistry Frontiers*, 2021, **5**, 6941-6950.
- [5] B.-Q. Li, L. Kong, C.-X. Zhao, Q. Jin, X. Chen, H.-J. Peng, J.-L. Qin, J.-X. Chen, H. Yuan, Q. Zhang and J.-Q. Huang, Expediting redox kinetics of sulfur species by

atomic-scale electrocatalysts in lithium–sulfur batteries, *InfoMat*, 2019, **1**, 533-541.